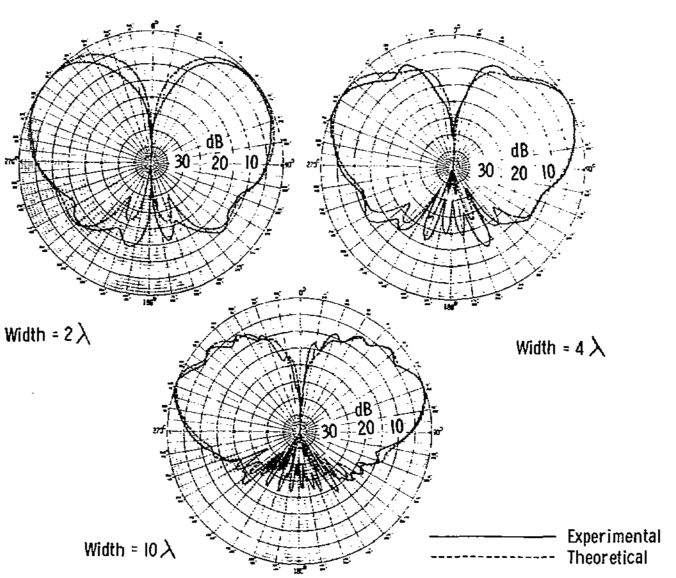

Fig. 2. Experimental and theoretical radiation pattern of λ/4 monopole over ground plane of various width.

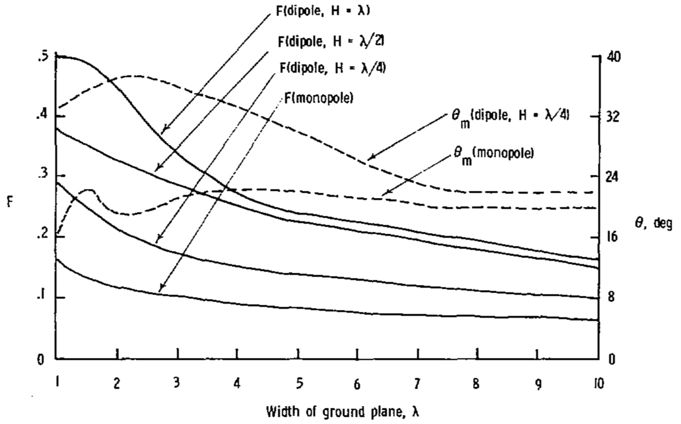

Fig. 3. Fraction F of power radiated in backward direction for various antenna configuration and ground plane. θ_m is angle of maximum radiation from ground plane.

The discrepancy between the measured and computed patterns in the backward direction may be attributed to two factors. Firstly, the diffraction field from the orthogonal edges have been neglected in computation but in practice it is large enough to influence the small field in the backward direction. Secondly, there is a small error in centering the dipole and the ground plane is not perfectly plane. One interesting point is that the shadowing by the ground plane is relatively insensitive to its width when it exceeds 5λ.

Acknowledgment

The author wishes to thank W. F. Croswell for many helpful discussions and B. W. Connor for assistance in measurement.

References

[1] M. Born and E. Wolf, *Principles of Optics*. London: Pergamon Press, 1965, pp. 556–592.
[2] T. B. A. Senior, "The diffraction of a dipole field by a perfectly conducting half-plane," *Quart. J. Mech. Appl. Math.*, Vol. VI, pt. 1, pp. 101–114, 1953.
[3] J. B. Keller, "The field of an antenna near the center of a large circular disk," *J. SIAM*, vol. 11, no. 4, pp. 1110–1112, 1963.
[4] D. L. Sengupta and V. H. Weston, "Investigation of the parasitic loop counterpoise antenna," *IEEE Trans. Antennas Propagat.*, vol. AP-17, pp. 180–191, Mar. 1969.
[5] R. W. Redlich, "Image radiation from a finite ground plane in two dimensions," *IEEE Trans. Antennas Propagat.*, (Commun.), vol. AP-16, pp. 334–337, May 1968.
[6] C. A. Balanis, "Analysis of an array of line sources above a finite ground plane," *IEEE Trans. Antennas Propagat.*, vol. AP-19, pp. 181–185, Mar. 1971.
[7] ——, "Radiation characteristics of current elements near a finite length cylinder," *IEEE Trans. Antennas Propagat.*, vol. AP-18, pp. 352–359, May 1970.
[8] P. H. Pathak and R. G. Kouyoumjian, "The dyadic wedge diffraction coefficient," ElectroScience Lab., Ohio State Univ., Columbus, Rep. RF 2183-4, June 1970.

Impedance Comparisons for the Asymmetrically Driven Thin Cylindrical Antenna

JOSEPH H. PIERLUISSI

***Abstract*—The results from various approximate methods of solution to three basic equations for the impedance of the asymmetrically driven perfectly conducting thin cylindrical antenna are briefly discussed and compared. Generally good agreement is found between method-of-moment solutions and the three-term King-Wu theory. Largest disagreement with those approximate methods is found with the Shen-Wu-King solution and the joining procedure.**

Introduction

Although the radiation characteristics of the asymmetrically driven thin cylindrical antenna have been known from experiments for several years, rigorous theoretical studies of the problem were most probably instigated by Hallén's analysis [1] of the center-driven case. For a perfectly conducting thin cylinder of radius a and length L extending from $z = -h_2$ to $z = h_1$ and excited by a Dirac delta voltage source of magnitude V_0 at $z = 0$, the basic equations adopted by succeeding workers to solve for the current I over the antenna surface may be written as:

$$\nabla\phi + j\omega A_z = V_0\delta(z) \tag{1}$$

$$\frac{j}{4\pi\omega\epsilon_0\mu_0}\left(\frac{\partial^2}{\partial z^2} + k^2\right)A_z = V_0\delta(z) \tag{2}$$

$$A_z = C\cos kz + D\sin kz - \frac{j^2\pi\mu_0 V_0}{\eta_0}\sin k|z|. \tag{3}$$

Here, the potentials A_z and ϕ are the solutions to the Helmholtz equations, k is the propagation constant at a frequency ω, ϵ_0 and μ_0 are the medium characteristic parameters, and C and D are constants to be determined from the end-condition $I(h_1) = I(-h_2) = 0$. Clearly, (3) follows from (2) by integration, and (2) follows from (1) with the use of the Lorentz gauge. For solution, the approximate kernel is used in connection with A_z and ϕ.

Numerical Solutions

The first practical solution to (3) was obtained by King and Wu [2] using an iterative procedure which lead to a three-term model for the current. Impedance calculations using the model were made by Harrison *et al.* [3], samples of which are shown under column (1) in Table I. The values missing on this table were not included in a similar table given in [3], in spite of the fact that the model is valid for the resonant lengths $L = 0.5\lambda$ and $L = 1\lambda$. A much older and less useful iterative solution by King [4] resulted in an "averaging" method for obtaining the impedance of an asym-

Manuscript received May 25, 1972; revised September 20, 1972. This work was supported in part by a Grant from the University Research Institute, University of Texas, El Paso.

The author is with the Department of Electrical Engineering, University of Texas, El Paso, Tex. 79968.

TABLE I

Impedance Values as Provided by Various Models

Total Length L	Arm Lengths		Radius X10^{-3} a	Input Impedance of Asymetrically-Driven Antennas Ω = 10						
	h_1	h_2		(1) King-Wu	(2) Shen-Wu-King	(3) Popović-Surutka	(4) Polynomial (3-terms)	(5) Sinusoidal (3-terms)	(6) Joining (Sinusoidal)	(7) Joining (King-Middleton)
0.29	0.18	0.11	1.93	18.74-j330.13	25.77-j341.80	17.6-j318.8	16.90-j301.46	16.92-j303.58	18.53-j297.37	20.11-j306.89
0.29	0.21	0.08	1.93	19.26-j397.35	24.41-j407.35	18.2-j377.4	17.50-j356.56	17.54-j358.99	24.45-j329.54	25.95-j341.10
0.35	0.25	0.10	2.36	34.30-j256.50	38.42-j249.66	33.4-j244.9	32.08-j229.87	31.99-j231.54	47.49-j196.90	48.59-j204.50
0.35	0.29	0.06	2.36	39.06-j365.41	40.09-j346.01	37.3-j336.2	35.91-j313.75	35.84-j315.77	71.61-j229-46	71.58-j245.72
0.35	0.32	0.03	2.36	- - - - - - -	24.03-j598.98	- - - - - -	39.42-j527.94	39.59-j531.00	115.01-j300.83	- - - - - - -
0.48	0.26	0.22	3.22	70.99+j6.82	68.24+j21.06	77.5+j7.1	74.02+j9.18	72.00+j7.99	74.18+j8.81	74.82+j8.87
0.48	0.27	0.21	3.22	73.43+j6.42	70.32+j21.31	79.9+j6.8	76.29+j9.02	75.16+j7.81	80.02+j11.09	80.17+j11.11
0.48	0.32	0.16	3.22	92.59+j3.23	87.53+j22.79	99.2+j3.7	94.97+j6.86	93.11+j5.54	128.98+j25.27	127.12+j25.23
0.48	0.34	0.14	3.22	105.05+j0.54	98.86+j23.20	111.7+j0.8	107.19+j4.66	104.77+j3.35	161.40+j30.27	159.07+j30.11
0.48	0.37	0.11	3.22	147.72-j12.69	136.86+j21.52	153.3-j13.2	147.47-j6.94	143.05-j7.75	266.07+j25.11	267.69+j22.39
0.48	0.38	0.10	3.22	184.23-j28.00	170.33+j19.84	187.3-j30.0	181.25-j21.90	175.06-j21.66	346.45-j1.03	351.74-j9.41
0.48	0.40	0.08	3.22	238.05-j61.97	219.44-j3.54	234.9-j62.6	228.93-j52.10	220.45-j49.29	442.44-j63.66	450.99-j84.91
0.48	0.42	0.06	3.22	316.09-j132.47	295.50-j29.53	298.0-j217.4	292.92-j114.55	282.61-j105.95	534.36-j181.55	538.89-j224.95
0.48	0.45	0.03	3.22	- - - - - - -	568.10-j327.28	- - - - - -	391.36-j469.30	400.75-j442.07	561.89-j539.70	- - - - - - -
0.50	0.25	0.25	3.37	- - - - - - -	77.18+j53.95	- - - - - -	86.72+j40.05	85.31+j38.78	85.31+j38.78	- - - - - - -
0.50	0.30	0.20	3.37	- - - - - - -	86.12+j57.71	- - - - - -	96.92+j41.96	95.07+j40.63	109.90+j47.63	- - - - - - -
0.50	0.32	0.18	3.37	- - - - - - -	99.29+j62.66	- - - - - -	111.96+j43.99	109.41+j42.62	146.41+j56.76	- - - - - - -
0.50	0.35	0.15	3.37	- - - - - - -	122.51+j69.83	- - - - - -	138.36+j45.41	134.46+j44.19	209.79+j62.47	- - - - - - -
0.50	0.37	0.13	3.37	- - - - - - -	163.73+j78.33	- - - - - -	184.49+j41.76	178.01+j41.52	312.77+j46.06	- - - - - - -
0.50	0.40	0.10	3.37	- - - - - - -	240.73+j81.87	- - - - - -	265.69+j16.36	254.88+j20.40	454.76-j39.32	- - - - - - -
0.50	0.42	0.08	3.37	- - - - - - -	391.71+j47.67	- - - - - -	392.44-j88.58	380.17-j70.07	565.83-j248.60	- - - - - - -
0.50	0.45	0.05	3.37	- - - - - - -	651.06-j170.18	- - - - - -	466.08-j377.10	480.81-j342.41	529.19-j515.52	- - - - - - -
0.50	0.48	0.02	3.37	- - - - - - -	746.94-j862.44	- - - - - -	299.43-j737.71	340.25-j737.11	387.78-j678.24	- - - - - - -
0.80	0.48	0.32	5.37	680.35-j290.17	743.45-j227.28	492.0-j369.0	442.81-j368.53	490.72-j368.94	393.43-j173.65	352.83-j159.19
0.80	0.57	0.23	5.37	75.07-j240.26	113.91-j259.76	89.8-j235.6	79.00-j217.11	83.23-j231.54	97.63-j202.81	97.65-j186.95
0.80	0.64	0.16	5.37	51.19-j209.98	60.84-j213.67	51.3-j198.2	45.13-j182.04	45.49-j192.96	47.25-j196.18	53.59-j190.77
0.80	0.69	0.11	5.37	50.00-j246.29	48.27-j230.51	42.9-j213.1	36.83-j195.56	36.01-j205.89	38.10-j195.00	43.46-j198.05
0.80	0.72	0.08	5.37	42.19-j320.74	42.51-j275.12	41.8-j251.7	34.19-j229.57	32.72-j240.22	42.59-j196.98	46.47-j210.84
0.96	0.50	0.46	6.45	801.56-j337.07	812.17-j288.62	470.2-j462.2	416.49-j435.55	454.42-j441.46	466.48-j490.74	418.92-j472.42
0.96	0.51	0.45	6.45	619.96-j219.40	682.92-j174.36	447.8-j345.2	414.30-j347.34	437.56-j347.95	481.76-j453.44	447.24-j430.41
0.96	0.54	0.42	6.45	362.93-j74.37	372.64-j25.53	320.6-j140.0	317.82-j135.98	316.01-j141.94	493.20-j281.07	481.40-j251.83
0.96	0.58	0.38	6.45	191.28-j31.68	217.09+j2.37	208.4-j58.0	210.48-j49.79	206.38-j59.99	396.74-j104.71	382.59-j69.08
0.96	0.61	0.35	6.45	132.40-j9.13	145.40+j6.10	144.7-j29.5	147.75-j21.99	144.40-j31.98	264.71-j26.23	247.32-j3.65
0.96	0.64	0.32	6.45	98.50-j16.58	108.86+j5.58	110.0-j18.1	113.19-j12.01	110.20-j21.12	168.35-j10.03	158.58-j1.11
0.98	0.57	0.41	6.60	287.59+j7.18	325.07+j49.80	332.9-j44.1	309.77-j59.05	302.15-j60.94	458.88-j227.31	448.87-j221.37
0.98	0.73	0.25	6.60	89.64+j22.34	86.69+j27.99	93.4+j28.5	96.74+j14.79	91.68+j6.90	90.83+j6.62	96.30+j24.63
1.00	0.50	0.50	6.74	- - - - - - -	669.10-j538.16	- - - - - -	287.21-j466.13	322.13-j488.50	322.13-j488.50	- - - - - - -
1.00	0.55	0.45	6.74	- - - - - - -	645.01-j85.91	- - - - - -	422.82-j282.43	442.80-j268.23	393.57-j415.89	- - - - - - -
1.00	0.60	0.40	6.74	- - - - - - -	278.89+j103.02	- - - - - -	293.76+j8.69	283.28+j 7.86	423.88-j150.39	- - - - - - -
1.00	0.70	0.30	6.74	- - - - - - -	106.49+j61.86	- - - - - -	122.01+j42.23	116.67+j34.81	135.23+j34.21	- - - - - - -
1.11	0.57	0.54	7.51	159.45-j404.82	268.16-j454.05	161.7-j364.5	134.82-j339.49	149.04-j362.42	145.82-j359.51	137.19-j320.67
1.11	0.59	0.52	7.51	196.54-j425.18	307.58-j459.10	183.9-j372.5	153.38-j347.30	170.28-j369.95	156.41-j358.85	145.78-j321.46
1.11	0.60	0.51	7.51	268.11-j441.54	380.87-j456.44	225.8-j382.2	188.24-j357.72	210.00-j378.94	174.87-j358.68	161.18-j321.98
1.11	0.62	0.49	7.51	370.05-j416.26	490.18-j421.52	291.8-j385.0	243.85-j364.06	272.54-j380.83	201.78-j351.12	184.90-j320.60
1.11	0.63	0.48	7.51	440.57-j293.54	612.03-j316.62	385.7-j361.9	322.63-j352.39	358.14-j358.77	237.54-j339.03	218.71-j314.22

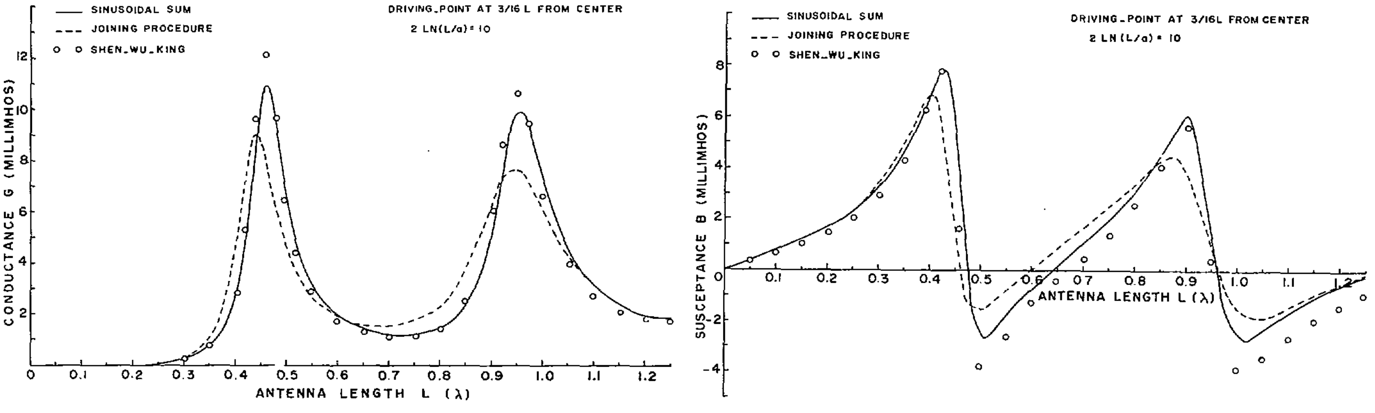

(a) (b)

Fig. 1. (a) Conductance of asymmetrically driven dipole. (b) Susceptance of asymmetrically driven dipole.

metrically driven antenna from the respective impedances of two center-driven antennas, having arm-lengths equal to each one of the arm-lengths of the asymmetric case. The method was called the "joining procedure" in [3] and used, together with the well-known King–Middleton model [5] for center-driven antennas, to generate the values listed in Table I under column (7).

If the first two terms to the right of (3) are discarded and the proper integration limits placed on A_z, it results in an integral equation for the current on an infinitely long antenna for which an exact integral solution is available [6]. The integral was evaluated in approximate analytical form by Shen *et al.* [7], and the results used to propose a three-term traveling-wave expression for the current. The model was used by the present author to calculate the impedance values given in Table I under column (2), as well as to generate the admittance curves of Fig. 1.

Popović [8] solved (3) with the method of moments assuming as basis function a current distribution in the form of polynomials in z, continuous over each antenna arm and forced to be equal at the driving-point. Using third-order polynomials and point-matching the present author computed the impedance values shown in Table I and under column (4). The center-driven case of (3) was studied by Neff *et al.* [9] using a three-term sinusoidal series for the current, defined over the entire antenna length, together with the method of moments and point-matching. The present author adopted their sinusoidal series for the current $I(z)$ and defined it over each antenna arm, that is,

$$I(z) = \begin{cases} \sum_{n=1}^{N} A_n \sin \frac{n\pi}{2h_1} (h_1 - z), & 0 \leq z \leq h_1 t \\ \sum_{n=1}^{N} B_n \sin \frac{n\pi}{2h_2} (h_2 + z), & -h_2 \leq z \leq 0 \end{cases} \tag{4}$$

to compute with the same procedure the impedance values shown in Table I under column (5) and the admittance curves of Fig. 1 labeled "sinusoidal sum." Furthermore, with the center-driven case of (3) and (4) and the joining procedure column (6) in Table I was prepared, as well as the admittance curves of Fig. 1 labeled "joining procedure."

Equation (2) was first used by Harrington and Mautz [10] in connection with the method of moments and point-matching, assuming a triangular- (as well as pulse-) subsectional basis function for the current. Unfortunately, the impedance tables referenced in [10] do not include the case $\Omega = 2 \ln (L/a) = 10$ used in the preparation of Table I and Fig. 1. Popović and Surutka [11] generalized the two-term variational procedure of Storer [12] to analyze (2). Their results are listed in Table I under column (3). Although values for the resonant lengths are missing in this column, the method is good for any kh_1 or kh_2 less than $3\pi/2$. A detail development of (1) for use with the method of moments and pulse basis-function expansion may be found in the book by Harrington [13].

DISCUSSION

A close examination of Table I reveals good agreement between the impedance values under columns (3), (4), and (5), all of which may be considered to be method-of-moments solutions. The agreement between these and the King-Wu values in column (1) is reasonable as a whole. The reactance components from the Shen–Wu–King model [column (2)], however, disagree significantly in some cases from the values given by the other two basic methods. The disagreement with a method-of-moments calculation (i.e., sinusoidal series) may be more clearly observed in Fig. 1. The poorer agreement between the previous results and the joining procedure, as seen both in column (6) and (7) and in Fig. 1, is to be expected since the latter is only a very approximate method. The curve labeled "sinusoidal sum" in Fig. 1 is in excellent agreement with [10, fig. 2]. Impedance calculations were made by the present author using (1) but they did not show significant difference with the other method-of-moments values. For instance, for the half-wave dipole with $L/2a = 200$ and 31 subsections, equation (1) gave an impedance of $85.26 + j43.21$, while Harrington and Mautz listed $86.4 + j45.4$ in [10].

All of the models described can provide impedance values for the center-driven antenna, but none can treat the end-driven case. Except for the joining and variational methods all can yield the current distribution along the antenna. All the current-distribution models excepting the model of Shen *et al.* make the initial assumption that the current vanishes at the antenna ends. By far the one requiring the least computational time for a given antenna is the model of Shen *et al.* This is in view of the fact that to use the attractive joining procedure advantageously one requires a nonexistent simple model for the center-driven case. It is recalled that a truncated-Fourier series fits the function described in a least-squares sense, and as such the accuracy of the representation depends on the location of the sampling points used in the analysis. For the reported computations with (4) the sampling points needed in the determination of A_n and B_n were evenly distributed along each antenna arm, with one sample taken always at the driving-point. A reasonable criterion to use with (4) is that the number of terms chosen be so that one of them have the period of the sinusoidal-current assumption for the specified length. Hence, the longest antenna that can be treated with three terms of (4) is the center-driven case of $L = 1.50\lambda$. This value is also the limiting length for the King–Wu model. Based on their [7, fig. 3], Shen *et al.* indicated that their model was good only for the cases where the driving point was farther than about 0.15λ from either antenna end. Calculations made by this author consistently gave reasonable values (see Table I) whenever $L \geq 0.3\lambda$ for a wide range of driving-point positions, the precise length being dependent on the antenna radius.

The impedance values in Table I are intended primarily to extend to seven cases the two-case comparison of Harrison *et al.* [3], thus updating their results with new models and with the presently used method-of-moment methods. Perhaps the only intelligent observation that can be made from the results given here, is that a comprehensive theoretical and experimental study is greatly needed to establish the accuracy of the several methods available for the impedance (and current distribution) of the asymmetrically-driven linear antenna.

ACKNOWLEDGMENT

The author wishes to thank Mr. J. W. Doll for his valuable assistance in programming some of the equations presented in this paper, and B. Hollander for typing the final manuscript. Special recognition is given to the reviewers, who through their criticism significantly improved this paper.

REFERENCES

[1] E. Hallén, "Theoretical investigations into the transmitting and receiving qualities of antenna," *Nova Acta Regiae Soc. Sci. Upsal.*, vol. 11, no. 4, pp. 1–44, 1938.

[2] R. W. P. King and T. T. Wu, "The cylindrical antenna with arbitrary driving-point," *IEEE Trans. Antennas Propagat.*, vol. AP-13, no 5, pp. 710–718, 1965.

[3] C. W. Harrison, C. D. Taylor, and E. A. Aronson, "On the driving-point impedance of an asymmetrical dipole," *IEEE Trans. Antennas Propagat.* (Commun.), vol. AP-14, pp. 794–795, Nov. 1966.

[4] R. W. P. King, "Asymmetrically-driven antennas and the sleeve dipole," *Proc. IRE*, vol. 38, pp. 1154–1164, Oct. 1950.

[5] R. W. P. King and D. Middleton, "The cylindrical antenna; current and impedance," *Quart. Appl. Math.*, vol. 3, no. 4, pp. 302–335, 1946.

[6] E. Hallén, "Exact treatment of antenna current wave reflection at the end of a tube-shaped cylindrical antenna," *IRE Trans. Antennas Propagat.*, vol. AP-4, pp. 479–491, May 1956.

[7] L. C. Shen, T. T. Wu, and R. W. P. King, "A simple formula for current in dipole antennas," *IEEE Trans. Antennas Propagat.*, vol. AP-16, pp. 542–547, Sept. 1968.

[8] B. D. Popović, "On polynomial approximation of currents along thin asymmetrical cylindrical dipoles," *IEEE Trans. Antenna Propagat.*, vol. AP-19, pp. 117–120, Jan. 1971.

[9] H. P. Neff, C. A. Siller and J. D. Tillman, "A simple approxiation to the current on the surface of an isolated thin cylindrical center-fed dipole of arbitrary length," *IEEE Trans. Antennas Propagat.*, vol. AP-18, pp. 399–400, May 1970.

[10] R. F. Harrington and J. R. Mautz, "Straight wires with arbitrary excitation and loading," *IEEE Trans. Antennas Propagat.*, vol. AP-15, pp. 502–515, July 1967.

[11] B. D. Popović and J. V. Surutka, "A variational solution to the problem of an asymmetrical cylindrical dipole," *IEEE Trans. Antennas Propagat.*, vol. AP-19, pp. 17–22, Jan. 1971.

[12] J. E. Storer, "Variational solution to the problem of the symmetrical cylindrical antenna," Croft Lab., Harvard Univ., Cambridge, Mass., Tech. Rep. 101, 1952.
[13] R. F. Harrington, *Field Computation by Moment Method.* New York: Macmillan, ch. 4, 1968.

Synthesis of Broad-Band Arrays with Arbitrary Frequency-Independent Elements

FRANC BRATKOVIČ

Abstract—**The application of dynamic programming to the synthesis of broad-band antenna arrays with arbitrary frequency-independent elements is investigated. Four criteria are proposed for the optimization of the array. By employing these criteria it is shown that the optimum array is the one with monotonic spacings. For such arrays the principle of optimality is proved and the limits, within which dynamic programming is applied, are analytically calculated. A 35-element array with ratio of upper-to-lower frequencies equal to 3 is synthesized by this method.**

INTRODUCTION

Grating lobes occur in the radiation pattern of a broad-band antenna array. Suitable spacing of elements reduces the grating lobes. The optimum configuration of element spacings in the broad-band sense is the one that produces minimal peak magnitude of the radiation pattern in the visible range outside the main lobe in the whole frequency band.

Ishimaru [1] transformed the radiation pattern into Poisson's sum. Ishimaru and Chen [2] reported that the radiated power of each grating lobe is equal to the radiated power of the main lobe, regardless of the spacing and the excitation of the elements. Applying stationary phase approximation Chow [3] synthesized the optimum nonuniform array of isotropic radiators. He also investigated the effect of the element pattern, and in turn reduced the first grating lobe of a narrow-band thinned array with an element pattern having a minimum coinciding with the first grating lobe.

A basically different approach to the synthesis of the optimum nonuniform arrays was purely numerical. Skolnik *et al.* [4] applied dynamic programming to nonuniform arrays, however, without proving the applicability of the principle of optimality. Since their method involved a wide range of possible spaces, quantization of the latter was coarse, to maintain computer time within reasonable limits.

In the present communication an analytical method is combined with dynamic programming in order to optimize broad-band arrays with arbitrary frequency-independent elements. Dynamic programming is applied to the array within analytically calculated boundary values. It is proved that the principle of optimality applies.

FORMULATION OF PROBLEM

A linear array (Fig. 1) of N nonuniformly spaced elements with radiation pattern $F_e(\Theta)$ can be described by two vectors, the complex current vector $I = (I_1,I_2,\cdots,I_N)$, and the real position vector $x = (x_1,x_2,\cdots,x_N)$. The radiation pattern of the array is

$$F_a(I,x,u) = F_e(u)F(I,x,u), \qquad u = \left(\frac{2\pi}{\lambda}\right)\sin\Theta \tag{1}$$

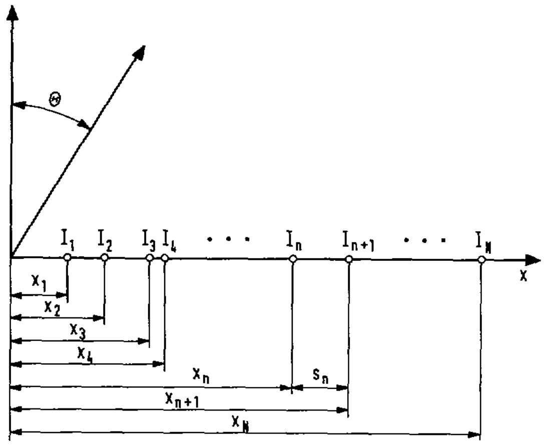

Fig. 1. Geometrical configuration of unsymmetrical nonuniform linear antenna array with N elements.

where the array factor is

$$F(I,x,u) = \sum_{n=1}^{N} I_n \exp(jx_n u). \tag{2}$$

The frequency-limit ratio of an antenna is the ratio between the highest and the lowest frequency at which the antenna still has the prescribed properties. In an antenna array the lowest frequency f_1 is limited by the minimum space $s_{\min}$, which must be no less than half the wavelength λ_1. The highest frequency f_2 is determined by the highest permissible boundary of the visible range u_{M2}. Thus the frequency-limit ratio is

$$R_f = \frac{f_2}{f_1} = \frac{s_{\min}u_{M2}}{\pi}. \tag{3}$$

The frequency-limit ratio of broad-band arrays depends mainly on the array factor. By introducing Poisson's summation formula, the array factor is transformed into

$$F(I,x,u) = \sum_{m=m_1(u)}^{m_2(u)} F_m(I,x,u) \tag{4}$$

$$F_m(I,x,u) = \int_{1/2}^{N+1/2} I(v)\exp\{j[ux(v) - 2m\pi v]\}\,dv.$$

Discrete variable n is substituted for by continuous variable v. Vectors I and x are substituted for by continuous functions $I(v)$ and $x(v)$ fulfilling conditions $I(n) = I_n$ and $x(n) = x_n$, $n = 1,2,\cdots,N$.

The term F_0 represents the main lobe, whereas the other terms F_m represent the grating lobes. The terms $m_1(u)$ and $m_2(u)$ are the limits of the significant terms. The set of the spaces $s_n = x_{n+1} - x_n$, $n = 1,2,\cdots,N-1$, can be also substituted for by continuous space function $s(v)$, which fulfills conditions $s(n) = s_n$, $n = 1,2,\cdots,N-1$. Using the stationary phase method [5] and the approximation $x'(v) = s(v)$ one finds the interval in which F_m is significant:

$$\frac{2m\pi}{s_{\max}} \le u \le \frac{2m\pi}{s_{\min}}. \tag{5}$$

The magnitude of the lobe within the interval is

$$|F_m(I,x,u)| = \frac{|I(v)|}{Nm^{1/2}}\left[\frac{s(v)}{s'(v)}\right]^{1/2}, \qquad v = v(u). \tag{6}$$

The variable v depends on u because of the stationary phase condition

$$us(v) - 2m\pi = 0. \tag{7}$$

Manuscript received June 5, 1972; revised September 15, 1972. This work was supported by the Boris Kidrič Research Foundation under Contract 205/193-70.
The author is with the Faculty of Electrical Engineering, University of Ljubljana, 61001 Ljubljana, Yugoslavia.